Lifetime and Multipolarity Measurements in Cs^{131}†

D. J. HOREN
U. S. Naval Radiological Defense Laboratory, San Francisco, California
and
Lawrence Radiation Laboratory, University of California, Berkeley, California

AND

J. M. HOLLANDER AND R. L. GRAHAM*
Lawrence Radiation Laboratory, University of California, Berkeley, California

(Received 9 March 1964)

With the use of the Berkeley $\sqrt{2}\pi$, iron-free, beta-ray spectrometer, the half-life of the 78.69-keV state in Cs^{131} has been measured as (9.6±0.3) nsec, and that of the 133.54-keV state has been redetermined as (9.3±0.3) nsec. An upper limit of ≤0.4 nsec has been found for the half-life of the 216.01-keV state. *L*-subshell ratios, and multipolarity assignments based thereon, are given for a number of transitions in Cs^{131}. A new transition with an energy of 969.1 keV has been observed, and the 461-keV transition was found to consist of a doublet with energies of 461.3 and 462.9 keV. The data indicate that the ground ($\frac{5}{2}+$) and 78.69-keV ($\frac{7}{2}+$) states of Cs^{131} probably arise from different intrinsic states ($d_{5/2}$ and $g_{7/2}$, respectively) upon which are based collective levels located at 123.73 and 133.54 keV. Tentative spin and parity assignments are included. Poor agreement is found with existing theoretical predictions.

I. INTRODUCTION

THE level structure of Cs^{131} is of interest because (1) it has not yet been explained satisfactorily on the basis of a particular nuclear model, and (2) Cs^{131} appears to lie between regions of spherical and deformed nuclear shapes.

Recently, Kelly and Horen[1] (hereafter referred to as KH) investigated the conversion electron spectrum of 11.5-day Ba^{131} which leads to levels in Cs^{131}. These authors proposed a decay scheme (see Sec. VI below) which encompassed most of the experimental data known at that time. In particular, they showed that the first excited state of Cs^{131} occurs at an energy of 78.6 keV, and tentatively assigned to this level a spin and parity $\frac{7}{2}+$. With such an assignment it was suggestive that the ground ($\frac{5}{2}+$) and first excited ($\frac{7}{2}+$) states of Cs^{131} were the analogs of the first excited ($\frac{5}{2}+$) and ground ($\frac{7}{2}+$) states of Cs^{133}, respectively.

In order to explore this possibility, we have measured the lifetime of the 78.6-keV state and the *E*2-*M*1 mixing ratio of the 78.6-keV transition. In addition, we have (1) made measurements of the lifetimes of other levels in Cs^{131}, (2) determined the mixing ratios of a number of transitions in Cs^{131}, and (3) have measured a number of transition energies to higher precision than had hitherto been done. The results of this work are the subject of the present paper.

II. EXPERIMENTAL METHOD

A sample of 11.5-day Ba^{131} was prepared by irradiating 1 mg of barium nitrate enriched [2] to 55.6% in Ba^{130} for 3 weeks in a neutron flux of 4.6×10^{14} n-cm^{-2} sec^{-1} at the Materials Testing Reactor (MTR), Arco, Idaho. The active material was dissolved in dilute nitric acid and transferred to a boat-shaped tantalum filament in which it was dried. Sources were prepared by subliming the material in vacuo through a 1- ×10-mm collimator on to a 7 mg-cm^{-2} Al foil backing.

The apparatus consisted of the Berkeley 50-cm radius iron-free spectrometer,[3,4] and fast coincidence circuitry which has been described elsewhere.[5] For scanning the electron conversion lines, the spectrometer electron detector was a Geiger counter with either a gold-coated Mylar (~960 μg-cm^{-2}) or a multilayer Formvar film (~100 μg-cm^{-2}) window. Counter window apertures of 1 mm wide×20 mm high and 5 mm wide×20 mm high were used in conjunction with baffle apertures corresponding to instrumental resolutions of ~0.05 and ~0.2% in momentum.

The lifetime measurements were performed with the spectrometer baffle aperture set for ~0.5% resolution in momentum, and the electron detector for these measurements was a 10-mm-wide×25-mm-high×1-mm-thick sheet of Naton 136 plastic phosphor optically coupled to a 14-stage CBS-1090 photomultiplier. A larger plastic phosphor mounted on a 14-stage RCA-6810A was placed behind the source to detect *K* x rays. A Lucite absorber was inserted between the source and x-ray detector in order to enhance the x-ray-to-background ratio. The time-to-height converter was calibrated[5] before and after each lifetime measurement and, typically, the stability was better than ~1% of the output pulse height.

† Work performed under the auspices of the U. S. Atomic Energy Commission.

* Permanent address: Physics Division, Atomic Energy of Canada Limited, Chalk River, Ontario, Canada.

[1] W. H. Kelly and D. J. Horen, Nucl. Phys. **47**, 454 (1963).

[2] Obtained from the Stable Isotopes Division, Oak Ridge National Laboratory, Oak Ridge, Tennessee.

[3] K. Siegbahn, C. L. Nordling and J. M. Hollander, Lawrence Radiation Laboratory Report UCRL-10023, 1962 (unpublished).

[4] J. M. Hollander and R. L. Graham, Lawrence Radiation Laboratory Report UCRL-10624, 1963 (unpublished).

[5] R. L. Graham, J. M. Hollander, and P. Kleinheinz, Nucl. Phys. **49**, 641 (1963).

TABLE I. Conversion electron intensities in the decay of 11.5-day Ba^{131}.

Electron energy (keV)	Conversion shell	Transition energy (keV)	Adopted transition energy (keV)	Relative electron intensities[b] This work	Kelly and Horen
18.865	K	54.839	54.84	29.9	
49.124	L_I	54.830		4.68	~3
49.474	L_{II}	54.834		20.4	20.4
49.825	L_{III}	54.839		26.0	25.6
42.713	K	78.687	78.69	65.6	55.7
72.976	L_I	78.682		9.22	5.7
73.334	L_{II}	78.694		0.86	0.7
73.682	L_{III}	78.696		0.25	<0.3
46.454	K	82.428	82.43	2.02	1.8
52.276	K	92.250	92.25	36.1	28.9
86.519	L_I	92.225		5.25	
87.765	K	123.739	123.73	1060	925
118.009	L_I	123.715		101	91
118.371	L_{II}	123.731		120	114
118.712	L_{III}	123.726		131	123
97.566	K	133.540	133.54	43.4	43
127.817	L_I	133.523		5.48	4.6
128.178	L_{II}	133.538		1.63	1.1
128.519	L_{III}	133.544		1.47	1.1
101.289	K	137.263	137.26	1.82	0.85
151.30	L_I	157.01	157.01	0.42	0.3
180.00	K	215.97	216.01	100	100
210.33	L_I	216.04		13.6	
a	L_{II}			0.98	
a	L_{III}			0.32	
203.59	K	239.56	239.56	9.85	9.16
233.85	L_I	239.56		1.19	
a	L_{II}			0.09	1.11
a	L_{III}			0.04	
210.86	K	246.83	246.83	2.52	
241.05	L_I	246.76		0.39	0.25
213.38	K	249.36	249.36	10.1	8.82
243.65	L_I	249.36		1.2	
a	L_{II}			0.13	1.23
a	L_{III}			0.04	
258.47	K	294.45	294.45	0.38	0.34
288.95	L	294.65[c]		0.06	
315.23	K	351.21	351.21	0.14	0.12
337.18	K	373.15	373.15	15.7	15.5
367.51	L_I	373.22		2.0	
a	L_{II}			0.26	3.08
a	K		404.3	1.04	
398.61	L_I	404.31		0.20	0.14
403.17	M	404.39		0.04	
391.71	K	427.68	427.7	0.09	0.06
415.71	K	451.69	451.7	0.04	0.3
425.28	K	461.25	461.3	0.10	0.05
426.91	K	462.88	462.9	0.11	
444.65	K	480.62	480.6	0.26	0.32
a	L_I	480.19		0.04	
450.62	K	486.55	486.6	1.0	1.04
481.04	L_I	486.75		0.15	0.11
485.55	M	486.76		0.05	
460.33	K	496.30	496.3	28.2	25.9
490.63	L_I	496.34		3.3	
a	L_{II}			0.18	3.56
a	L_{III}			0.046	
495.31	M	496.53		0.86	0.72
549.09	K	585.06	585.1	0.46	0.42
579.48	L_I	585.19		0.065	0.06
584.26	K	620.23	620.2	0.37	0.32
796.07	K	832.04	832.0	0.039	0.04
888.39	K	924.36	924.4	0.092	0.09
918.60	L_I	924.31		0.015	0.01
923.24	M	924.46		0.004	
933.09	K	969.06	969.1	0.004	
1012.21	K	1048.19	1048.2	0.13	0.12
1042.37	L_I	1048.07		0.018	0.01
1046.64	M	1047.85		0.005	

[a] The energy has been calculated from the transition energy in order to carry out the intensity analysis.
[b] Intensities arbitrarily normalized to 100 for K 216.01.
[c] The L_I line has been used to calculate the transition energy. Assuming a pure $E2$, a "weighted" L binding energy would give 294.45 keV.

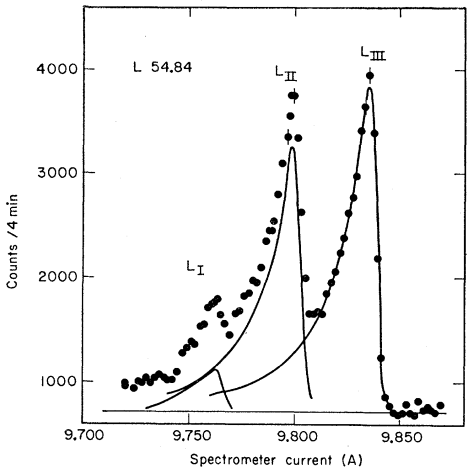

FIG. 1. L internal-conversion electron spectrum of 55.84-keV transition in Cs^{131}.

III. INTERNAL CONVERSION ELECTRON SPECTRUM

At the time that this work was done, the stability of the magnetic field and the current measuring apparatus of the spectrometer was usually sufficient to allow momentum determinations to better than 2 parts in 10^4. In a few cases, however, the measurements were accurate to only about 8 parts in 10^4. Absolute energy measurements were made by utilizing a Cs^{137} source ($B\rho = 3381.08 \pm 0.30$ G cm)[6] to determine the spectrometer constant (i.e., $B\rho$ divided by I). With the Cs^{137} source occupying one position in the source holder and the Ba^{131} source the other, the $K661.60$ Cs and $K216.01$ Ba lines were measured successively. The sources were then simultaneously rotated 180° and the line positions again determined. The average of the line positions determined from the rotated and nonrotated source positions was used to determine the energy of the $K216$ line in Ba^{131} decay relative to the standard line. Whenever the source, counter window aperture or baffle aperture was changed, the $K216.01$ line was remeasured in order to check the spectrometer constant.

The energies and relative intensities of the internal conversion electron lines measured in this investigation are summarized in Table I. In most cases, the energies are believed to be accurate to better than 0.05% and the relative intensities to about 15%. The uncertainties in the relative intensities are due in part to the corrections for source decay (we used a half-life of 11.5 days for Ba^{131}), and the use of different sources, counter window apertures and baffle apertures.

The intensities of the low-energy electron lines (less

[6] R. L. Graham, G. T. Ewan and J. S. Geiger, Nucl. Instr. Methods **9**, 245 (1960).

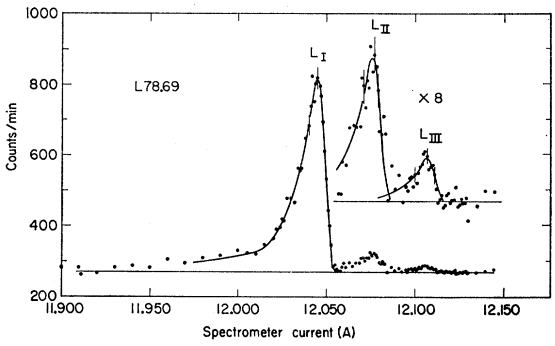

FIG. 2. L internal-conversion electron spectrum of 78.69-keV transition in Cs^{131}.

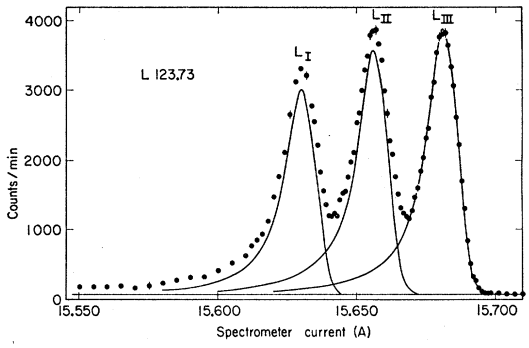

FIG. 3. L internal-conversion electron spectrum of 123.73-keV transition in Cs^{131}.

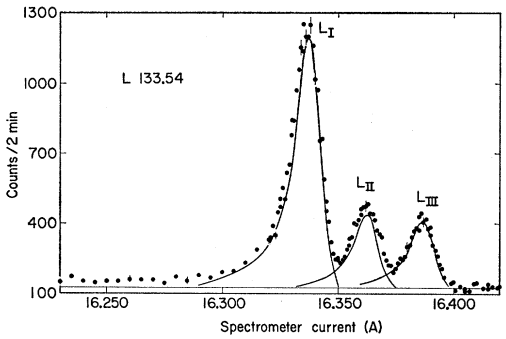

FIG. 4. L internal-conversion electron spectrum of 133.54-keV transition in Cs^{131}.

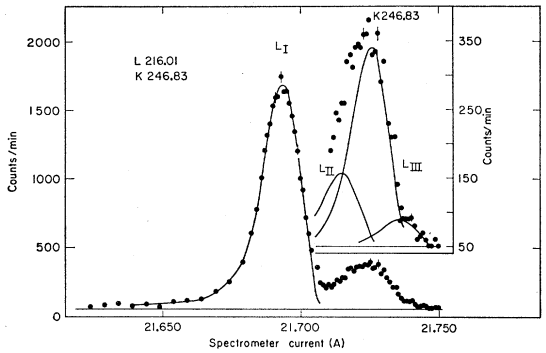

FIG. 5. L internal-conversion electron spectrum of 216.01-keV transition in Cs^{131}.

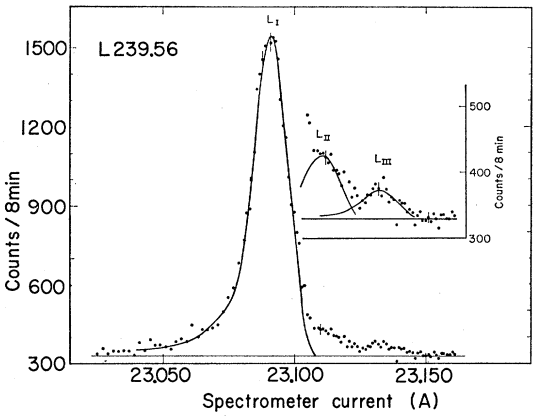

FIG. 6. L internal-conversion electron spectrum of 239.56-keV transition in Cs^{131}.

than 100 keV) were corrected for absorption in those measurements for which a Mylar window was used with the Geiger counter. No corrections were thought necessary for measurements taken with the formvar window (~97% transparent to 40-keV electrons). Also, included in Table I are the relative intensities given in KH. With few exceptions, the agreement is seen to be quite good.

As we were unable in this work to observe the L_{II} and L_{III} lines of the 92.25-keV transition, it is unlikely that Kelly and Horen[1] actually detected these lines in the permanent magnet spectrographs. (See "Remarks" in Table I of their paper.) The poor agreement among the relative intensities in the region of 450 keV is probably explained by the fact that the background density on the photographic plates from the permanent magnet spectrographs changed abruptly in the vicinity of the $K452$ line. This caused Kelly and Horen[1] to overestimate the intensity of this line, which in turn affected their quoted intensities of the $K427$ and $K461$ lines.

Our more accurate energy determinations clearly indicate that the line assigned in KH as $K324$ is predominantly the $L294$. Analysis showed that the pres-

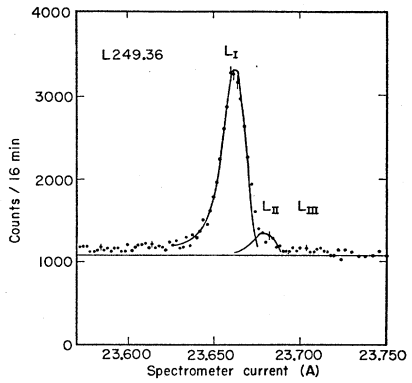

FIG. 7. L internal-conversion electron spectrum of 249.36-keV transition in Cs^{131}.

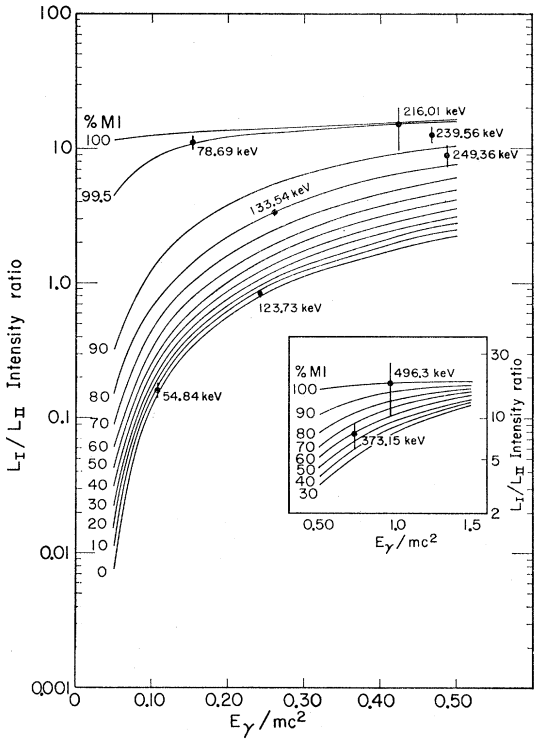

FIG. 8. Comparison of experimental L_I/L_{II} subshell ratios with theoretical values obtained from the tables of Sliv and Band for various $E2/M1$ admixtures.

ence of a $K323.5$ line could account at most for about 10% of the intensity of this line. The $K461$ line was found to be composite, and was resolved into two lines with energies of 461.3 and 462.9 keV. Both lines can be accommodated by the decay scheme shown in Fig. 16. A previously unobserved weak transition of 969.1 keV was also detected in this work.

IV. *L*-SUBSHELL RATIOS AND MULTIPOLARITY ASSIGNMENTS

In Figs. 1–7, the L-conversion electron spectra for a number of transitions in Cs^{131} are shown. The shapes of near-lying single conversion lines were used, when necessary, in the analyses of these data. The experimentally determined L-subshell ratios are compared in Figs. 8 and 9 with the theoretical values as calculated by Sliv and Band.[7] Multipolarity assignments for these transitions are summarized in Table II. Also included in this table are assignments for the 92.25- and 294.45-keV transitions. The $\geq 80\%$ $M1$ character assigned to the 92.25-keV transition follows from the fact that we did not observe its L_{II} line. A 20% $E2$ admixture would have made this line observable.

The 294.45-keV transition is tentatively assigned

TABLE II. Multipolarity assignments of transitions in Cs^{131}.

Transition energy (keV)	Multipolarity
54.84	$92\pm8\%$ $E2$
78.69	$99.5\pm0.4\%$ $M1$
92.25	$>80\%$ $M1$
123.73	$95\pm5\%$ $E2$
133.54	$80\pm2\%$ $M1$
216.01	$>91\%$ $M1$
239.56	$94\pm4\%$ $M1$
249.36	$86\pm8\%$ $M1$
373.15	$56\pm16\%$ $M1$
496.3	$>80\%$ $M1$

multipolarity $E2$ because: (1) The experimentally determined K/L ratio was measured as 5.9, which is to be compared with theoretical values of 5.6 and 7.6 for a pure $E2$ or $M1$ transition, respectively. (2) With the assumption that this transition is pure $E2$, the broad shape of the observed L line could be reconstructed with the use of a near-lying single conversion line. We cannot, of course, exclude a possible $M1$ admixture.

To investigate the possible presence of transitions between the 123.73-keV state and the 78.69- and 133.54-keV states, a search was made in the regions corresponding to $L45.04$ and $M9.81$ lines. In each case, the conversion spectra were flat within the statistical accuracy.

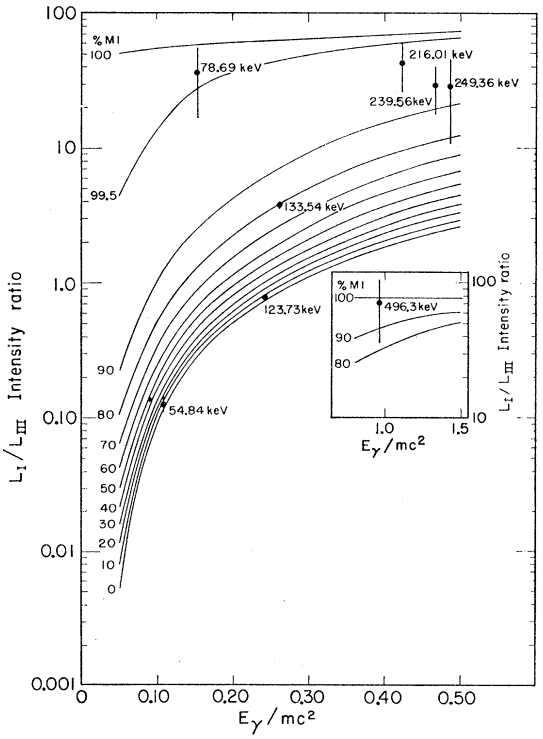

FIG. 9. Comparison of experimental L_I/L_{III} subshell ratios with theoretical values obtained from the tables of Sliv and Band for various $E2/M1$ admixtures.

[7] L. A. Sliv and I. M. Band, Leningrad Physico-Technical Institute Report, *Table of Internal Conversion Coefficients of Gamma-Rays* (Academy of Science USSR, Leningrad, 1958).

V. LIFETIME MEASUREMENTS AND GAMMA-RAY EMISSION PROBABILITIES

A. Lifetime of the 123.73-keV State

To measure the lifetime of the 123.73-keV state, the spectrometer current was adjusted to focus the $K123.73$ electron line, and the detector behind the source was set to record K x rays. The $K123.73$–K x-ray delay curve (background subtracted) is shown in Fig. 10. The prompt component arises from the simultaneous detection of a K electron and its corresponding K x ray. The raw data above channel ~140 were analyzed by a least squares computer program (IBM-7090) to fit the expression $A+B\exp(-\lambda t)$. After including an allowance for the uncertainty in the time calibrations we find as a best value for the half-life of the 123.7-keV state

$$T_{1/2}(123.73)=3.7\pm0.1 \text{ nsec.}$$

The $K92.25$–K x-ray delay curve (see Fig. 11) showed the same half-life. In this figure, the slope above channel 140 was probably caused by coincidences between background electrons (see insert), upon which the $K92.25$ line is superimposed, and K x rays. The predominant source of this background is the tail of the $K123.73$ line. Hence, it is not surprising that, within the statisti-

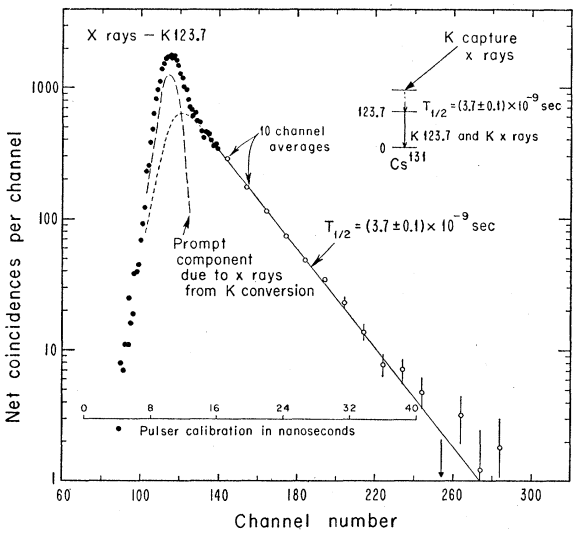

FIG. 10. $K123.73$–K x-ray delayed coincidence spectrum (background subtracted). Increasing pulse height above the prompt position represents electrons delayed relative to x rays.

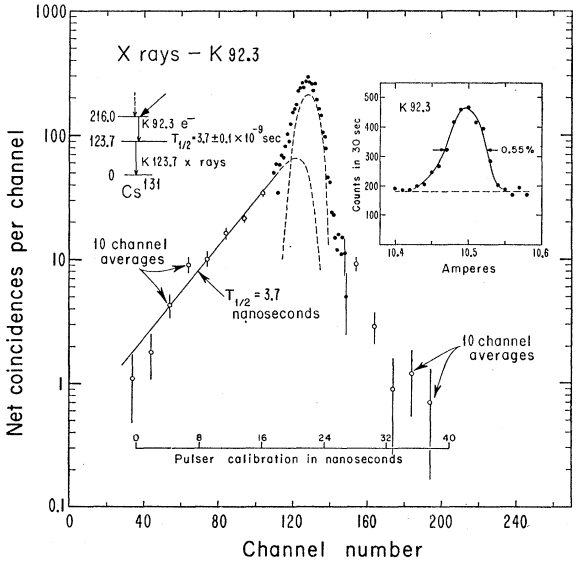

FIG. 11. $K92.25$–K x-ray delayed coincidence spectrum (background subtracted). Increasing pulse height below the prompt position represents x rays delayed relative to electrons.

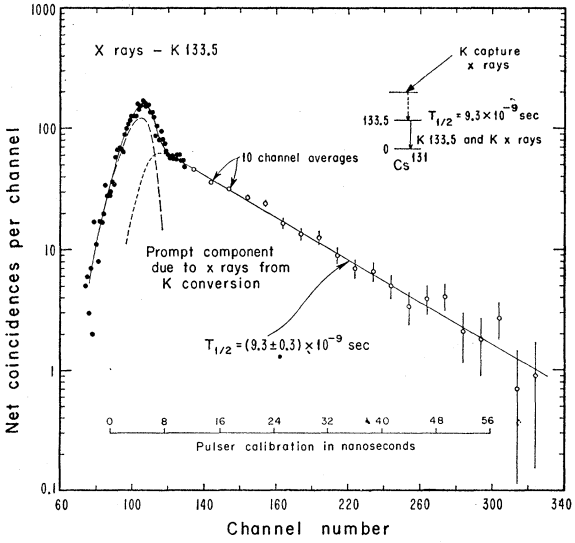

FIG. 12. $K133.54$–K x-ray delayed coincidence spectrum (background subtracted). Increasing pulse height above the prompt position represents electrons delayed relative to x rays.

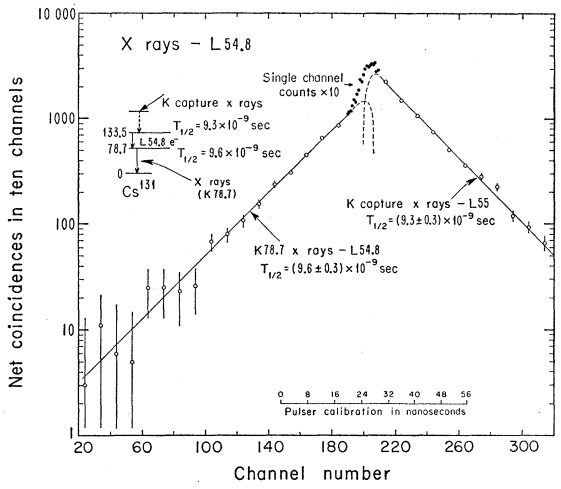

FIG. 13. $L54.84$–K x-ray delayed coincidence spectrum (background subtracted). Increasing pulse height above the prompt position represents electrons delayed relative to x rays.

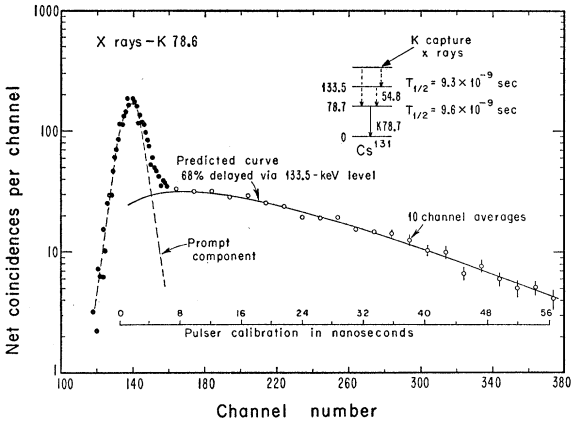

FIG. 14. $K78.69$–K x-ray delayed coincidence spectrum (background subtracted). See text for discussion.

cal errors, this slope is also consistent with a half-life of 3.7 nsec.

Our value of 3.7±0.1 nsec for the half-life of the 123.73-keV state is in good agreement with those reported by other workers.[8]

B. Lifetime of the 133.54-keV State

In Fig. 12 is shown the delay curve obtained by recording coincidences between the $K133.54$ electron line and K x rays. Analysis of the data above about channel 135 yielded a half-life for the 133.54-keV state of

$$T_{1/2}(133.54)=9.3\pm0.3 \text{ nsec.}$$

Coincidences between K x rays and the $L54.84$ electron line gave a similar value (see Fig. 13, the portion of the curve above channel 210).

Using scintillation detectors, Bodenstedt *et al.*[9] and Kelly and Horen[1] have obtained for this half-life values of 13.3±0.5 and 12.7±1.0 nsec, respectively. These are about 30% higher than our result. This difference may be due to the fact that in the scintillation measurements the width of the energy selecting channels was such as to measure the lifetimes of the 123.73- and 133.54-keV states simultaneously, so that a compound decay curve was obtained, with the 13-nsec component much weaker than the 3.7-nsec component. In this work, the higher resolution of the spectrometer allowed us to select in one channel radiation from only the 133.54-keV state, and a single decay curve with an improved true-to-chance ratio was obtained.

C. Lifetime of the 78.69-keV State

The $L54.84$–K x-ray delayed coincidence spectrum is shown in Fig. 13. Since the spectrometer was set to detect L electrons there is no prompt component in this spectrum due to K x rays corresponding to the focused conversion electrons. In this figure, the direction of increasing pulse height (to the right of the prompt position, ~channel 205) corresponds to electrons delayed in time relative to x rays, and (as mentioned in the previous section) that portion of the curve represents a measurement of the lifetime of the 133.54-keV state. Delay to the left (i.e., toward lower channel number) signifies coincidences in which the K x rays are delayed relative to $L54.84$ electrons. From an analysis of the latter portion of the curve, we obtain for the half-life of the 78.69-keV state

$$T_{1/2}(78.69)=9.6\pm0.3 \text{ nsec.}$$

The $K78.69$–K x-ray time spectrum was also measured, and is shown in Fig. 14. Reference to the decay scheme (Fig. 16) indicates that this delay curve should be composed of the following three components: (1) Prompt coincidences with x rays following K conversion of the 78.69-keV transition. (2) K x rays associated with the direct feeding of the 78.69-keV state. These x rays arise from the K capture and K conversion (the latter contribution is negligible here) which precede such transitions as well as from the K conversion of such transitions themselves. The delay spectrum resulting from such coincidences is a decaying exponential with half-life corresponding to that of the 78.69-keV state. (3) K x rays from K capture and K conversion which are associated with population of the 133.54-keV state. These are in coincidence with $K78.69$ electrons via the 54.84-keV transition. Because of the measureable half-life of

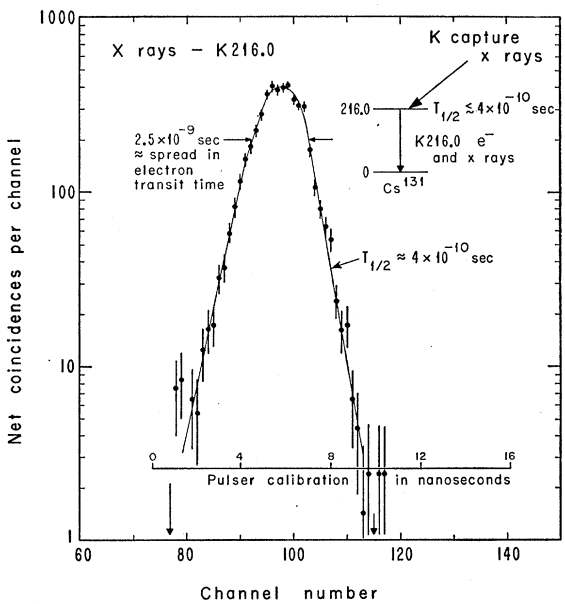

FIG. 15. $K216.01$–K x-ray delayed coincidence spectrum (background subtracted). Increasing pulse height above the prompt position represents electrons delayed relative to x rays.

[8] *Nuclear Data Sheets*, compiled by K. Way *et al.* (Printing and Publishing Office National Academy of Sciences–National Research Council Washington, 25, D. C.), NRC 61-2-48.

[9] E. Bodenstedt, H. J. Körner, C. Günter, D. Hovestadt, and J. Radeloff, Nucl. Phys. **20**, 557 (1960).

TABLE III. Gamma-ray emission probabilities.

Transition energy (keV)	$T(M1)$ Expt $(sec)^{-1}$	$T(E2)$ Expt $(sec)^{-1}$	$T(M1)$ Theory $(sec)^{-1}$	$T(E2)$ Theory $(sec)^{-1}$ S.F.$=1$	Expt/theory $M1$	Expt/theory $E2$
54.84–92.0% $E2$	1.10×10^{5}	1.26×10^{6}	4.65×10^{9}	2.49×10^{4}	2.4×10^{-5}	51
78.69–99.5% $M1$	2.58×10^{7}	1.30×10^{5}	1.37×10^{10}	1.51×10^{5}	1.9×10^{-3}	0.86
92.25–>80.0% $M1$	$\geq3.65\times10^{7}$		2.18×10^{10}		$\geq1.7\times10^{-3}$	
123.73–95.0% $E2$	4.97×10^{6}	9.46×10^{7}	5.35×10^{10}	1.45×10^{6}	9.3×10^{-5}	65
133.54–80.0% $M1$	2.55×10^{7}	6.38×10^{6}	6.75×10^{10}	2.15×10^{6}	3.8×10^{-4}	3.0
216.01–~100% $M1$	$\geq1.44\times10^{9}$		2.24×10^{11}		$\geq6.4\times10^{-3}$	

the 133.54-keV state, this situation gives rise to a growth-and-decay curve. Only the contributions from (2) and (3) are important in the region beyond channel 170 (see Fig. 14). Utilizing the decay scheme as shown in Fig. 16, our measured lifetimes for the 78.69- and 133.54-keV levels, and the intensities of the transitions populating these levels, one can calculate the expected $K78.69$–K x-ray time spectrum for the region beyond the prompt component. The results of such a calculation are indicated by the solid curve in Fig. 14.

D. Lifetime of the 216.01-keV State

A I 216.01–K x-ray time spectrum has also been measured (Fig. 15). From the slope of the delay curve we can set an upper limit for the half-life of the 216.01-keV state as

$$T_{1/2}(216.01)\leq0.4 \text{ nsec}.$$

E. Gamma-Ray Emission Probabilities

From the lifetime and multipolarity information as determined in this work, one can calculate the partial $M1$ and $E2$ gamma-ray emission rates for the transitions originating from the 78.69-, 123.73-, and 133.54-keV levels. Lower limits can also be placed on the emission rates for the 216.01- and 92.25-keV transitions. In Table III, the calculated partial $M1$ and $E2$ gamma-ray emission probabilities are compared to the theoretical values as computed from the Moszkowski single particle formula[10] (with nuclear radius $r=1.2\times10^{-13}\times A^{1/3}$ cm). In most cases, total conversion coefficients were calculated from the experimental multipolarities with use of the theoretical conversion coefficient tables of Sliv and Band,[7] in conjunction with the experimentally determined $L/M+N$ ratios. The ratios of the

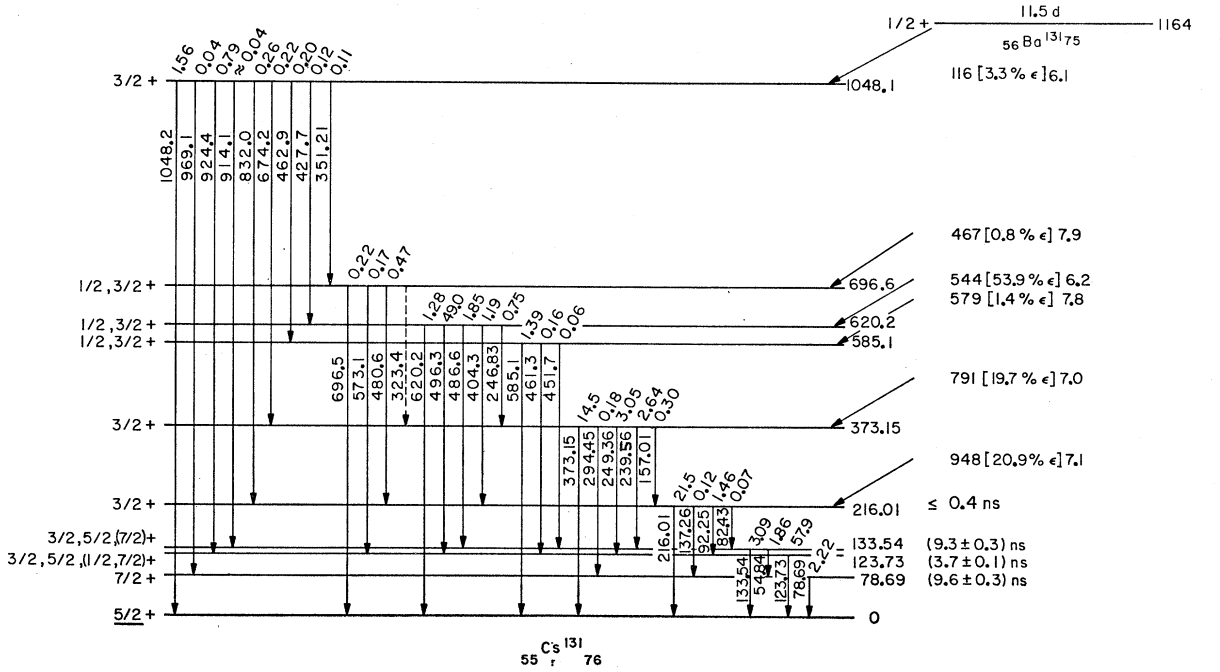

FIG. 16. Decay scheme for 11.5-day Ba^{131}. All energies are given in keV, the percent electron capture within the brackets, and the log ft values to the right of the percent branchings. Spins contained within parenthesis cannot be excluded, but are thought improbable. See text for discussion.

[10] S. A. Moszkowski, in *Beta and Gamma-Ray Spectroscopy*, edited by K. Siegbahn (North-Holland Publishing Company, Amsterdam, 1955), Chap. 13.

TABLE IV. Comparison of gamma-ray emission probabilities of the transitions between the first excited and ground states of Cs^{131} ($\frac{7}{2}+ \rightarrow \frac{5}{2}+$) and Cs^{133} ($\frac{5}{2}+ \rightarrow \frac{7}{2}+$).

Transition energy			$T(M1)$	$T(E2)$	$T(M1)$	$T(E2)$	Statistical factor[a]		Expt/theory	
Nucleus	(keV)	Multipolarity	Expt $(\text{sec})^{-1}$		Theory $(\text{sec})^{-1}$ S.F.$=1$		$M1$	$E2$	$M1$	$E2$
Cs^{131}	78.69	99.5% $M1$ 0.5% $E2$	2.58×10^{7}	1.30×10^{5}	1.37×10^{10}	1.51×10^{5}	1.29	0.143	1.46×10^{-3}	6
Cs^{133}	80.99	97.4% $M1$ 2.6% $E2$	3.98×10^{7}	1.02×10^{6}	1.49×10^{10}	1.81×10^{5}	1.71	0.190	1.56×10^{-3}	30

[a] See Ref. 9.

experimental to theoretical transition rates are given in the last two columns of Table III.

VI. DISCUSSION

A. Decay Scheme

The decay scheme of 11.5-day Ba^{131} as proposed in KH but modified to include the results of this investigation is shown in Fig. 16. The theoretical conversion coefficients of Sliv and Band were used to calculate the relative gamma-ray intensities. For the cases in which the multipolarity of a transition was not known, a 50% $M1-E2$ admixture was assumed. Except for the 157-keV transition, the gamma-ray intensities so obtained are in good agreement with those quoted in KH. The conversion electron data as given in KH were utilized for those transitions which were not measured in this work. The 323.4-keV transition is shown dotted as we were unable to confirm its existence.

The total decay energy has been reported by Robinson to be 1164-keV,[11] and this value has been used to calculate the log ft values. Using the K x-ray data of KH, we find that within the experimental errors there is no electron capture to the 78.69-keV state, and negligible (if any) capture to the ground, 123.73-, and 133.54-keV states. Were there capture to the latter two states, the log ft values for these transitions would be greater than 8.0 and 9.0, respectively.

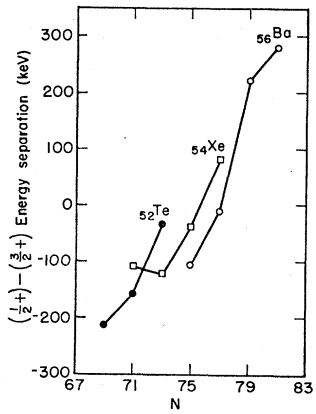

FIG. 17. Energy separation of the $\frac{1}{2}+$ and $\frac{3}{2}+$ levels of odd-A Te, Xe, and Ba isotopes as a function of the neutron number.

[11] B. L. Robinson, Bull. Am. Phys. Soc. **7**, 541 (1962).

B. Spin and Parity Assignments

78.69-keV State

On the basis of systematics of the energy splitting between the $\frac{5}{2}+$ and $\frac{7}{2}+$ levels in the odd-A cesium isotopes and the predominantly $M1$ character of the 78.69-keV transition, Kelly and Horen tentatively assigned the spin and parity of the 78.69-keV state as $\frac{7}{2}+$. The lifetime and multipolarity determinations of this work allow one to compare the gamma-ray emission probabilities of the 78.69-keV transition ($\frac{7}{2}+ \rightarrow \frac{5}{2}+$) to those for the analogous transition in Cs^{133} ($\frac{5}{2}+ \rightarrow \frac{7}{2}+$). The results of such a comparison are given in Table IV. That the $M1$ emission probabilities are nearly equal (column 10) when the statistical factor (column 8) is included is interpreted as additional support for the $\frac{7}{2}+$ assignment to the 78.69-keV state in Cs^{131}, as well as an indication that the major composition of the respective levels in Cs^{131} and Cs^{133} are similar.

The $E2$ emission probabilities, on the other hand, seem to indicate a difference in the components of the wave functions responsible for the small $E2$ components.

123.73-keV State

The L-subshell ratios, as determined in this work, indicate that the 123.73-keV transition consists of a 95% $E2+5\%$ $M1$ admixture. This is consistent with the results of gamma-ray correlation experiments,[7,12] which have shown that the angular distributions of cascades involving the 123.73-keV state are nonisotropic.

On the basis of these data, a spin and parity assignment of $\frac{1}{2}+$ to the 123.73-keV state would be excluded. However, in excluding such an assignment, we note the following reservations: (1) The extreme values of the L-subshell ratios for the 123.73-keV transition allowed by the experimental errors do not completely rule out the possibility that it is pure $E2$. (2) The angular correlation data might be subject to re-evaluation in the light of the more recent information on the decay of Ba^{131}.

Subject to the foregoing reservations, the possible spin and parity assignments for the 123.73-keV state are $\frac{3}{2}+$, $\frac{5}{2}+$, or $\frac{7}{2}+$.

[12] E. Bodenstedt, private communication cited in Ref. 1.

133.54-keV State

The presence of an $M1$ component in the 133.54-keV transition restricts the possible spin and parity assignments for the level at this energy to $\frac{3}{2}+$, $\frac{5}{2}+$, or $\frac{7}{2}+$. A $\frac{3}{2}+$ assignment would be excluded by the possible presence of an $M1$ component in the 54.84-keV transition. While our data cannot rule out such a possibility, it should be noted that within the errors it is consistent with a pure $E2$ assignment.

Other Spin Assignments

In discussing the assignments for the remaining levels in Cs^{131}, we assume a spin and parity of $\frac{1}{2}+$ for the ground state of Ba^{131}. Although the latter has not yet been measured, the systematic trend of the energy separation between the $\frac{1}{2}+$ and $\frac{3}{2}+$ levels in the odd-A Te, Xe, and Ba isotopes (see Fig. 17) appears to support such an assignment. From this assumption and the fact, established by Kelly and Horen, that the transitions in Cs^{131} involve no change in parity, it follows that the levels in Cs^{131} that are populated by electron capture have spins and parities of $\frac{1}{2}+$ or $\frac{3}{2}+$. Since the ground state spin and parity of Cs^{131} is known to be $\frac{5}{2}+$, the $M1$ character of the 216.01- and 373.15-keV transitions uniquely determines the assignments to the levels at these energies as $\frac{3}{2}+$. Such an assignment to the 373.15-keV level would require that the 294.45-keV transition be pure $E2$, and, as previously noted, this is indicated by the data. The observance of a transition between the 1048.2- and 78.69-keV states determines the spin and parity of the former as $\frac{3}{2}+$.

Interpretation of Angular Correlation Data

In our discussion of the interpretation of the angular correlation data of Bodenstedt's group,[12] we assume the validity of the $\frac{1}{2}+$ assignment to the ground state of Ba^{131} and also of the conclusions derived therefrom in the preceding subsection. [Of course, this discussion is also subject to comment (2) in the subsection pertaining to the 123.73-keV state.] We summarize here the conclusions derived from combining their data with the information obtained in this work.

The nonisotropic correlations of the 924–124 and 496–124 cascades rule out the assignment $\frac{1}{2}+$ for the 123.73-keV state. Furthermore, a $\frac{7}{2}+$ assignment is not compatible with the assignment of $\frac{3}{2}+$ to the 1048.1-keV state, nor with a $\frac{1}{2}+$ or $\frac{3}{2}+$ assignment to the 620.2-keV state. Hence, the spin and parity of the 123.73-keV state is restricted to the choices $\frac{3}{2}+$ or $\frac{5}{2}+$.

A $\frac{7}{2}+$ assignment to the 133.54-keV state would not be consistent with the correlation data involving the 587–134 cascade. An assignment of $\frac{1}{2}+(\frac{3}{2}+)$ to the 620.2-keV level would rule out $\frac{5}{2}+(\frac{3}{2}+)$ for the 133.54-keV state.

The data for the 832–216 and 404–216 cascades are consistent with $\frac{3}{2}+$ assignments to the 1048.2- and 216.01-keV states, and $\frac{1}{2}+$ or $\frac{3}{2}+$ to the 620.2-keV state.

VII. CONCLUSIONS

Utilizing the data available prior to the work of Kelly and Horen, Person and Rasmussen[13] attempted to explain the level structure of Cs^{131} in terms of the asymmetric rotor model (as applied to odd-mass nuclei) of Davydov and Fillippov.[14] The calculations of Person and Rasmussen were based in part upon spin assignments $\frac{1}{2}+$ and $\frac{7}{2}+$ for the 123.73- and 133.54-keV states, respectively. As previously noted in KH (and indicated here) such assignments seem unlikely. In view of this, as well as the fact that the data suggest more states with spins $\frac{1}{2}$ or $\frac{3}{2}$ than predicted by their calculations, it does not appear that a detailed comparison with the results of Person and Rasmussen is justifiable here.

Recently, Kisslinger and Sorensen have calculated the low-lying states in Cs^{131} as part of a detailed study of spherical nuclei.[15] With use of a two-body force consisting of a pairing force and a long-range component represented by a quadrupole force, these authors performed an intermediate coupling calculation which included all admixed states containing up to two phonons. For Cs^{131} they found that the lowest state has spin $\frac{5}{2}+$ and is predominantly an admixture of a $d_{5/2}$ single-particle state and the coupling of this level to a single-phonon excitation. The first excited state is predicted to lie at about 80 keV, and to arise predominantly from the coupling of a $d_{5/2}$ particle to a single-phonon excitation to form a total spin $\frac{1}{2}+$. Up to an energy of about 1 MeV no other levels with spin $\frac{1}{2}+$ and only two with spin $\frac{3}{2}+$ are predicted. Hence, the results of Kisslinger and Sorensen do not appear to explain satisfactorily the present information on the levels of Cs^{131}. Furthermore, the results of these authors indicate that the quadrupole strength is stronger in Cs^{131} than in Cs^{133} (see the tabulated wave functions in Ref. 15). Sorensen[16] has shown, that the effect of this should be to make the reduced $E2$ probability of the $d_{5/2}-g_{7/2}$ l-forbidden $M1$ transition in Cs^{131} larger than that of the analogous transition in Cs^{133}. As shown in Table IV, however, our results indicate that the $E2$ strength in Cs^{131} is only about one-fifth of that in Cs^{133}.

From Table III we see that for a statistical factor of unity the transition probability of the $E2$ component of the 78.69-keV transition is nearly equal to the single particle value. This appears to support the suggestion

[13] L. W. Person and J. O. Rasmussen, Nucl. Phys. **36**, 666 (1962).

[14] A. S. Davydov and G. F. Fillippov, Zh. Eksperim. i Teor. Fiz. **35**, 440 (1958) [English transl.: Soviet Phys.—JETP **8**, 305 (1959)].

[15] L. S. Kisslinger and R. A. Sorensen, Rev. Mod. Phys. **35**, 853 (1963).

[16] R. A. Sorensen, Phys. Rev. **133**, B281 (1964).

in KH that the 78.69-keV and ground states probably arise from different intrinsic levels ($g_{7/2}$ and $d_{5/2}$, respectively). As previously noted in KH, the relative strengths of the $E2$ components of the 54.84- and 133.54-keV transitions (see Table III) seem consistent with this interpretation, as does our nonobservance of a transition between the 133.54- and 123.73-keV states.

With the exception of the 373.15-keV state, the remaining levels in Cs^{131} seem to decay preferentially to the ground and 123.73-keV states. Since the 216.01- and 92.25-keV transitions are mainly $M1$, it appears that the 216.01-keV state cannot be interpreted as a collective level based upon the ground state. A definitive statement as to the origin of this state therefore cannot be made at this time.

ACKNOWLEDGMENTS

The authors would like to thank J. A. Harris for his assistance with the source preparation, and C. J. Butler, S. Clark, P. Salz and D. McClure for their ceaseless efforts to improve the reliability of the iron-free spectrometer during its early operating phases, in which time this work was performed. Stanley Klein (a 1963 summer student at USNRDL) was helpful in analyzing portions of the data. One of us (DJH) is grateful to BUSHIPS for support during part of this work. It is a pleasure for two of us (DJH and RLG) to extend our thanks to Dr. I. Perlman for the kind hospitality afforded us throughout our stay with the Nuclear Chemistry Division of the Lawrence Radiation Laboratory.

PHYSICAL REVIEW VOLUME 135, NUMBER 2B 27 JULY 1964

Electron Screening Corrections to Beta-Decay Spectra*

LOYAL DURAND, III
Physics Department, Yale University, New Haven, Connecticut

(Received 12 March 1964)

The corrections to the Fermi function $F(Z, W)$ which arise from the screening of the Coulomb field of the nucleus by the atomic electrons have been investigated using a Hulthén model for the screened field. The resulting problem is exactly solvable for the Schrödinger and Klein-Gordon equations. The results agree with those obtained by Rose and by Longmire and Brown using a modification of the WKB method, and disagree markedly with those obtained by Reitz by numerical integration of the Dirac equation. The latter results appear to be incorrect. The screening corrections are sufficiently small for light nuclei as not to affect materially present tests for the universal Fermi interaction and conserved vector current hypotheses for beta decay, but may become significant for low-energy beta transitions in heavy nuclei.

I. INTRODUCTION

THE wave function for a free electron of moderate energy is well approximated in the vicinity of an atomic nucleus by the wave function appropriate to a pure Coulomb field. This approximation leads to the appearance of the Fermi factor $F^{\pm}(Z,W)$ for a Coulomb field in the electron spectrum for allowed beta decay,

$$dN(W)=\tfrac{1}{2}m^5\pi^{-3}|M|^2F^{\pm}(Z,W)pW(W_0-W)^2dW, \quad (1)$$

where

$$F^{\pm}(Z,W)=2(1+s)(2pR)^{2s-2} \times e^{\mp\pi\eta}|\Gamma(s+i\eta)|^2[\Gamma(2s+1)]^{-2}. \quad (2)$$

In these expressions, W is the total energy and $p=[W^2-m^2]^{1/2}$ is the momentum of the electron, and W_0 is the maximum electron energy possible in the decay. The Coulomb parameter $Z\alpha W/p$ is denoted by η, while $s=[1-Z^2\alpha^2]^{1/2}$. The units are such that $\hbar=c=1$. This result for the electron spectrum is subject to many small corrections, including the effects of forbidden transitions, the finite spacial extension of the wave function of the decaying nucleon, the finite electromagnetic size of the nucleus, radiative electromagnetic corrections, and the effects of the screening of the Coulomb field of the nucleus by the outer electrons. Most of these corrections are well understood for light nuclei.[1] However, the electron screening corrections calculated by different methods are not consistent. These corrections have been investigated by Rose[2] and by Longmire and Brown[3] using a modified WKB approximation. The corrections were found to be rather small at moderate energies for light nuclei. Quite disparate results were obtained by Reitz[4] by numerical integration of the Dirac equation using a Thomas-Fermi-Dirac model for the interaction between the electron and the residual ion. The discrepancies are especially large in the high-energy, low-Z region in which the WKB method should

* Supported in part by the National Science Foundation.

[1] L. Durand, III, L. F. Landovitz, and R. B. Marr, Phys. Rev. **130**, 1188 (1963). The known corrections to the f values for the $0+\rightarrow 0+$ transitions in light nuclei are summarized in Table I of this paper.
[2] M. E. Rose, Phys. Rev. **49**, 727 (1936).
[3] C. Longmire and H. Brown, Phys. Rev. **75**, 264, 1102E (1949).
[4] J. R. Reitz, Phys. Rev. **77**, 10 (1950).